ENGINEERING TRANSACTIONS • *Engng. Trans.* • **60**, 4, 315–332, 2012
Polish Academy of Sciences • Institute of Fundamental Technological Research (IPPT PAN)
National Engineering School of Metz (ENIM)
SIXTY YEARS OF THE ENGINEERING TRANSACTIONS

Controller Concept for a Highly Parallel Machine Tool

Christoph HABERSOHN, Friedrich BLEICHER

Vienna University of Technology
Institute for Production Engineering and Laser Technology
Landstraßer Hauptstraße 152, 1030 Wien, Austria
e-mail: habersohn@ift.at

Modern high performance cutting processes force high demands on new machine tool concepts with enhanced mechanical stability and better dynamic behavior. In the development of innovative machine tool concepts the main focus is still set on the design of mechanical structures with parallel kinematics. The new machining center "X-Cut" consists of a double scissor kinematic structure with a degree of parallelism of two, incorporating four drives for the XY-plane movement. Thus, the arrangement of four interlinked axes leads to an over-determined kinematic structure. Due to the complex behavior of the kinematic structure a new method in NC-controller design and parameterization is needed, including enhanced compensation and preloading algorithms.

Key words: machine tools, kinematic structure, parallel kinematics, control design, modeling, simulation.

1. Introduction

For more than 15 years, machine tools based on parallel kinematics have become more important in manufacturing and handling applications. In fact, the machine tool industry has great expectations in the development of this type of machine structure; especially with respect to criteria such as stiffness, acceleration, accuracy, and the advantage of realizing similar assembly parts. Regarding the number of similar mechanical components that have to be assembled, a remarkable effect on the economic efficiency in building up machine tools has been anticipated. Experience resulting from the practical application of parallel kinematics settled because the development of various machine tools fell short of expectations due to disadvantages coming along with the non-linear behaviour of the mechanical structure in the overall workspace envelope. Many prototypes of machine tool concepts offer static stiffness in one preferred axis of more than 100 N/µm. The values of stiffness in the axes perpendicular to

the orientation of the struts drop down to very low levels of rarely more than 10 N/μm [1, 2].

High performance cutting processes puts a high demand on the concept of new machine tools with improved mechanical stability and better dynamic behaviour. As a result of this, the main focus is set on the design of machine tool structures with parallel kinematics. The first types of machine tools based on parallel kinematics were built with a degree of parallelism of one, e.g. Quickstep and Quickstep Neon [3]. This implies that there are as many drives in the machine as there are degrees-of-freedom offered for the tool and the Tool Centre Point (TCP) respectively [2].

In order to overcome restrictions in mechanics due to non-linear behaviour, a new approach has been found with a highly parallel design representing a kinematic structure offering a degree of parallelism of two, called "X-Cut" [4, 5]. The main kinematic structure offers two degrees of freedom of motion, and hence it allows in-plane movements. This kind of movement can already be performed by a scissor-type of kinematic structure, e.g. the DynaM, as presented in [6]. In order to get preloads into all kinematic transmission elements the scissor kinematic has to be doubled, thus the "V"-shape of the structure design becomes an "X"-shape, and gives the name to the invention. Due to the over-determined kinematic structure, it is possible to influence the preloading of all kinematic transmission elements during machining and feed motion. Furthermore, the basic stiffness of the entire structure can be improved. Applying a preload also affects the structure's damping characteristics whereby vibrations, which are introduced into the structure by reaction forces of acceleration and deceleration due to positioning motion of the main spindle as well as time variant processing forces, fade away much faster [4].

As a main focus of research, this innovative machine tool concept affords a new type of control algorithm because, in addition to the standard NC-controlled motion, it is necessary to integrate in the NC-control a strategy and control-functionality to handle and optimize the pretensioning forces. Hence, adaptive compensation methods have to be implemented with respect to motion and processing demands [7–11].

2. Hardware

The following figure illustrates the machine tool concept "X-Cut", with a 2D-overdetermined kinematic structure highlighted in the colour red. The third degree of motion is allocated in the work-piece slide. The control unit and the drives were provided by the Austrian control system vendor, Bernecker & Rainer [5].

To realize a minimum CPU cycle time of 800 μs, an APC 620 is used with a PP480 CNC panel in terminal mode as a HMI. The positioning of servo drives is

FIG. 1. Machine tool concept X-Cut.

controlled by five ACOPOSmulti and a 30 kW spindle by an ACOPOS. These servo motor controllers have a cyclic bus time of 400 µs. In addition to the internal absolute encoder of the drives, each axis has a Heidenhain glass linear scale mounted at the carriage to gain increased position accuracy [12].

3. Software

The machine tool NC-control is based on the Generic Motion Control software of Bernecker & Rainer. The system is configured with a virtual Cartesian coordinate system which is coupled with the real axis by an inverse transformation. The real TCP position is calculated by the virtual axis using a direct transformation of the physical axis. Regarding the software structure in this way, all positioning movements are defined by the Cartesian axes system and the physical axes follow the set points. The motion path itself is generated by the positioning requests directly to the virtual axes or by the NC kernel "ARNC0"

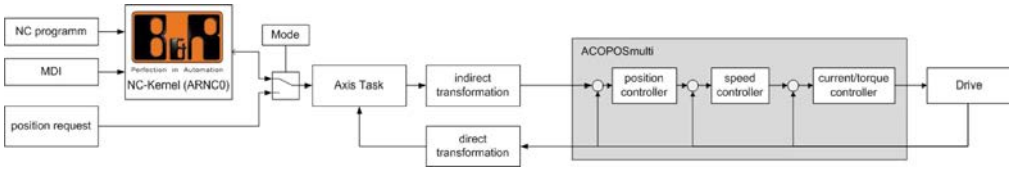

FIG. 2. Indirect and direct transformation.

which interprets G-code based on DIN 66025 from a NC-file or the input of the MDI. In any case, the position request is updated every 800 µs [12].

The ACOPOSmulti works with a three-layer controller architecture. In addition to the main positioning PI-controller, a secondary speed-controller and a third torque controller is subordinated. Each controller can be adjusted separately by the proportional band, the integral time and an offset, which can be altered at runtime with the active axis control.

3.1. Direct transformation

The direct transformation calculates the X-, Y-, and Z-position of the TCP in the workspace envelope using the real axis position. This is necessary for the control task to interpret position requests in an accurate way and send the real position to the HMI and the ARNC0. In fact, only the X- and the Y-positions have to be calculated, whereas the virtual Z-axis is defined by the position measure of the axis $Q5$ in the physical system.

For the calculation of the TCP-position, only the positions of two axes are necessary. Thus in the first version of implementation, axes one and two were used (see Fig. 3). To get a more symmetric situation an arrangement of op-

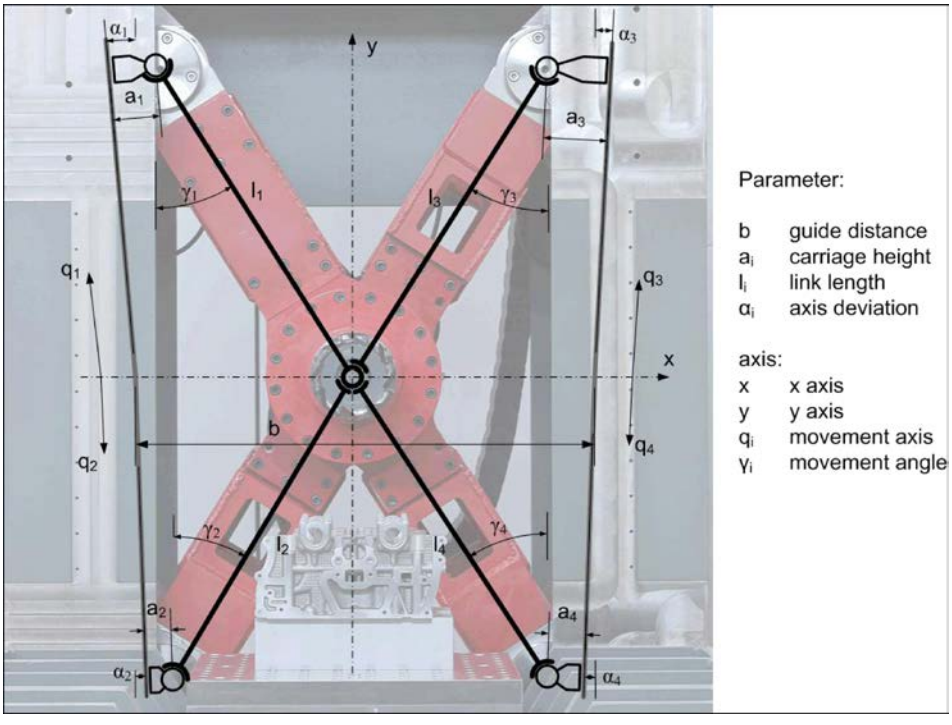

FIG. 3. Machine tool structure of X-Cut and kinematic parameters.

posing axes has been used in a second version by taking axes one and three in the position control loop. The following equations represent the direct coordinate system transformation, where C_1 and C_2 are calculated as two constants representing the geometrical dimensions as described in Fig. 3.

$$C_1 = b + q_1 \sin(\alpha_1) - a_1 \cos(\alpha_1) - a_3 \cos(\alpha_3) + q_3 \sin(\alpha_3),$$

$$C_2 = q_1 \cos(\alpha_1) + a_1 \sin(\alpha_1) - a_3 \sin(\alpha_3) - q_3 \cos(\alpha_3),$$

$$\beta = \arcsin\left(\frac{l_1^2 - l_3^2 + C_1^2 + C_2^2}{2l_1\sqrt{C_1^2 + C_2^2}}\right) - \arctan\left(\frac{C_2}{C_1}\right),$$

$$x = -\frac{b}{2} - q_1 \sin(\alpha_1) + a_1 \cos(\alpha_1) + l_1 \sin(\beta + \alpha_1),$$

$$y = q_1 \cos(\alpha_1) + a_1 \sin(\alpha_1) - l_1 \cos(\beta + \alpha_1),$$

$$z = q_5.$$

3.2. Indirect transformation

An indirect transformation is used to calculate the positional set-points of the real axes $Q1$–$Q5$ based on the X-, Y-, and Z-positions. The indirect transformation is very important to realize a closed loop position control in the NC-controller. The following equations describe the determination for each axis.

Axis $Q1$:

$$x = -\frac{b}{2} - q_1 \sin(\alpha_1) + a_1 \cos(\alpha_1) + l_1 \sin(\gamma_1),$$

$$y = q_1 \cos(\alpha_1) + a_1 \sin(\alpha_1) - l_1 \cos(\gamma_1),$$

with

$$R = x + \frac{b}{2} - a_1 \cos(\alpha_1),$$

$$S = y - a_1 \sin(\alpha_1),$$

$$q_1 = S\cos(\alpha_1) - R\sin(\alpha_1) + \sqrt{\left(S\cos(\alpha_1) - R\sin(\alpha_1)\right)^2 + (l_1^2 - R^2 - S^2)}.$$

Axis $Q2$:

$$x = -\frac{b}{2} + q_2 \sin(\alpha_2) + a_2 \cos(\alpha_2) + l_2 \sin(\gamma_2),$$

$$y = -q_2 \cos(\alpha_2) + a_2 \sin(\alpha_2) + l_2 \cos(\gamma_2),$$

with

$$R = x + \frac{b}{2} - a_2 \cos(\alpha_2),$$

$$S = y - a_2 \sin(\alpha_2),$$

$$q_2 = -S\cos(\alpha_2) + R\sin(\alpha_2) + \sqrt{(S\cos(\alpha_2) - R\sin(\alpha_2))^2 + (l_2^2 - R^2 - S^2)}.$$

Axis $Q3$:

$$x = \frac{b}{2} + q_3 \sin(\alpha_3) - a_3 \cos(\alpha_3) - l_3 \sin(\gamma_3),$$

$$y = q_3 \cos(\alpha_3) + a_3 \sin(\alpha_3) - l_3 \cos(\gamma_3),$$

with

$$R = -x + \frac{b}{2} - a_3 \cos(\alpha_3),$$

$$S = y - a_3 \sin(\alpha_3),$$

$$q_3 = S\cos(\alpha_3) - R\sin(\alpha_3) + \sqrt{(S\cos(\alpha_3) - R\sin(\alpha_3))^2 + (l_3^2 - R^2 - S^2)}.$$

Axis $Q4$:

$$x = \frac{b}{2} - q_4 \sin(\alpha_4) - a_4 \cos(\alpha_4) - l_4 \sin(\gamma_4),$$

$$y = -q_4 \cos(\alpha_4) + a_4 \sin(\alpha_4) + l_4 \cos(\gamma_4),$$

with

$$R = -x + \frac{b}{2} - a_4 \cos(\alpha_4),$$

$$S = y - a_4 \sin(\alpha_4),$$

$$q_1 = -S\cos(\alpha_4) + R\sin(\alpha_4) + \sqrt{(S\cos(\alpha_4) - R\sin(\alpha_4))^2 + (l_4^2 - R^2 - S^2)}.$$

The indirect transformation of the Z-axis is realized in a serial arrangement concerning the design of mechanical structure. Hence, the transformation can be calculated easily, and is equal to the position measure on the physical axis.

Axis $Q5$:

$$q_5 = z.$$

3.3. Parameter identification

To enhance the accuracy of the transformation, the real geometrical dimensions of the machine tool structure where determined by comparison of theoretically calculated and actually given position of the TCP by the use of redundant measurement devices. To minimize complexity, the carriage height is set to the theoretical value of the construction. Thereby the parameters: link length, guide distance and movement angle were determined, as well as the deviation in the X-axis of the not parameterised system.

4. Controller strategies

Regarding the concepts of position controller, two types of controller strategies can be distinguished.

4.1. Control system with four position controlled axes

In this arrangement four axes of the parallel kinematics structure are in a positioning control loop, called 4P-controller, as illustrated in Fig. 4. This type of strategy imposes a higher demand on the machine calibration because even a small position inaccuracy leads to high forces in the structure and in the drives. Due to an inaccuracy in the determination of real geometry, deviations between the real and the ideal kinematics arise. Thus, no power reserve exists for move-

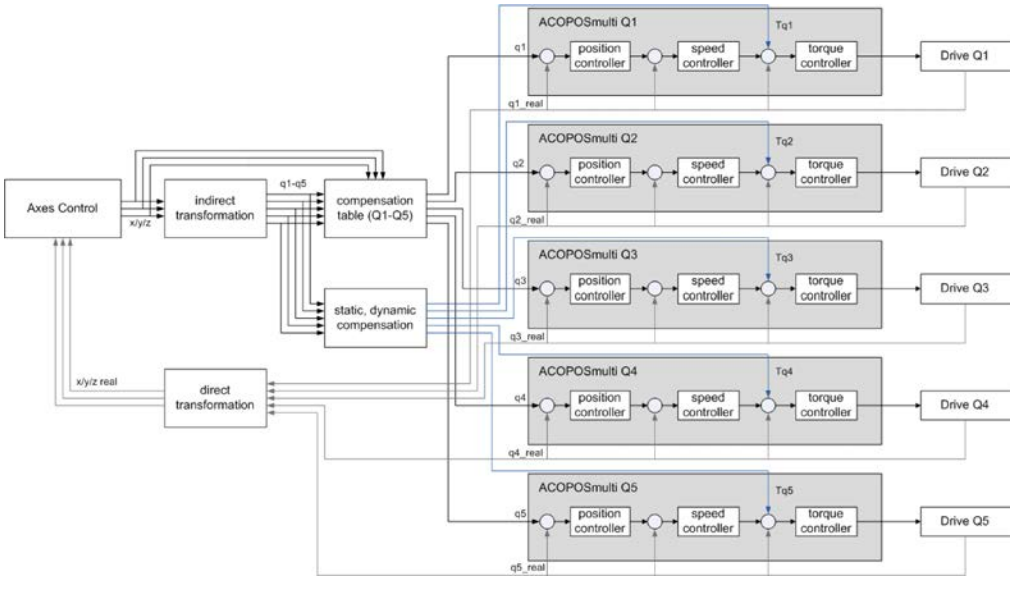

Fig. 4. Control strategy using four position controlling loops in the kinematics structure.

ment in the case of imprecise compensation. By high speed movements especially, even minor inaccuracies in the mechanical system generate huge torques in the drives and lead to overcharge of the drives.

An advantage is that all drives indicate the positioning movement and therefore the maximum torque of all drives can be used for the acceleration. Additionally the indicated forces of the cutting process are carried by all axes which enhance the machine stiffness behaviour.

4.2. Control system with two position and two force controlled axes

A second type of control strategy is based on the use of two axes, which are in position control loops, and two other axes, which are driven by a force control loop (see Fig. 5). Thus, the positioning of the TCP is done by two of the four axes and the other two axes tense the kinematic with a predefined force. The advantage of this system is focussing on the effect that geometrical inaccuracies are widely eliminated in the influence on the closed loop motion control.

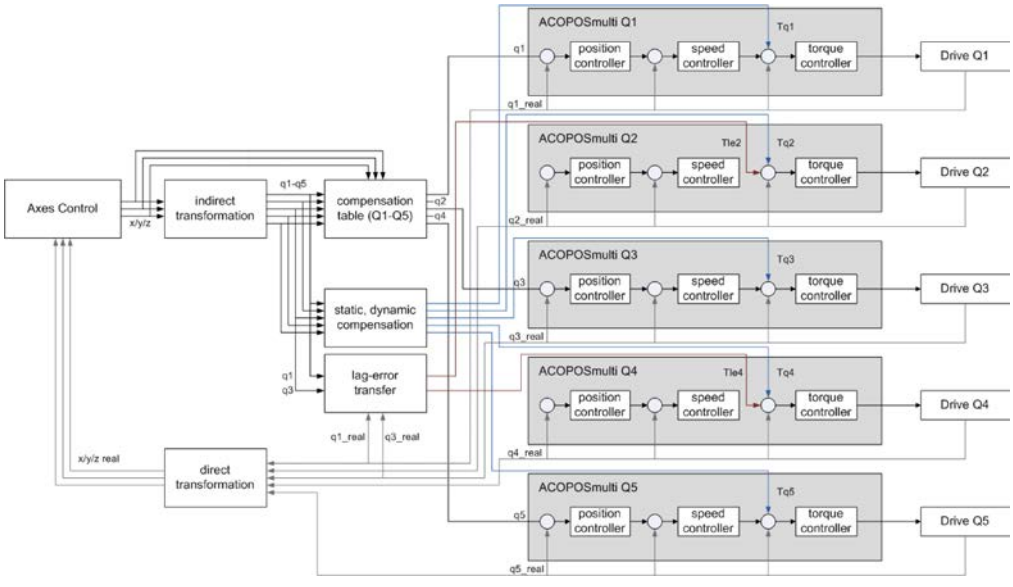

FIG. 5. Control strategy using two position controlling and two force controlling loops.

On the other hand, the force driven struts are not able to carry unknown external process forces, which lead to higher positioning inaccuracies as shown by the 4P controller strategy. Furthermore, the preloading forces had to be adjusted with respect to the movement, which generates higher demands on the control unit.

5. Compensation

To fulfil today's machining demands on positioning accuracies different compensation algorithms are implemented in the machine control.

5.1. Axis inaccuracies

In order to implement compensation functionality in the NC-controller the deviations of the real positioning motions to the reference values has been measured. Every 50 mm in square of the XY-working plane the deviations of the axes position in comparison to the calculated positions were measured by a mechanical 3D-measuring device. Based on these correction values a linear planar interpolation depending on the X- and Y-position is calculated for each axis and charged to the calculated position values (see Fig. 6).

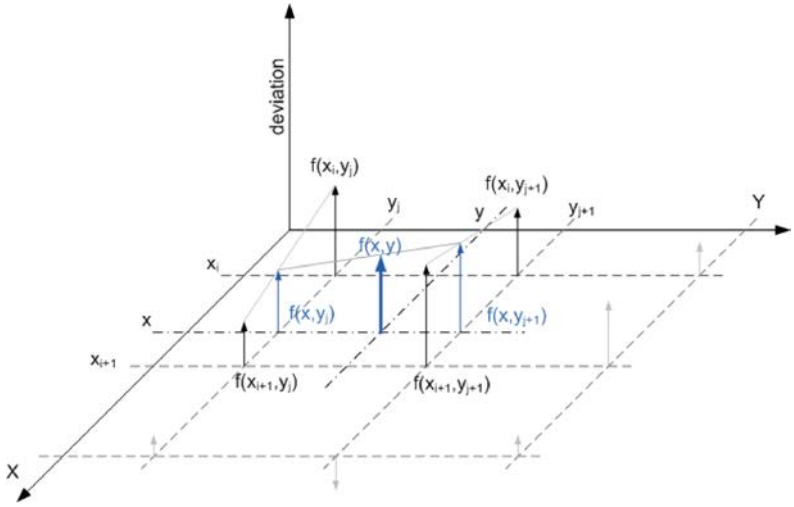

Fig. 6. Compensation of position inaccuracies.

The planar linear interpolation can be calculated in two steps.

$$f(x_i, y_j) \qquad \text{with discrete} \qquad x_0 - x_n, \quad y_0 - y_n.$$

Linear interpolation:

$$f(x, y_j) = f_{i,j} + \frac{f_{i+1,j} - f_{i,j}}{x_{i+1} - x_i}(x - x_i),$$

$$f(x, y_{j+1}) = f_{i,j+1} + \frac{f_{i+1,j+1} - f_{i,j+1}}{x_{i+1} - x_i}(x - x_i).$$

Linear interpolation in the X- and Y-axes:

$$f(x,y) = f(x,y_j) + \frac{f(x,y_{j+1} - f(x,y_j)}{y_{j+1} - y_j}(y - y_j).$$

5.2. Static and dynamic compensation

The compensation is based on Newton's axioms. To minimize the computing time the masses of each slide and the rods are modelled as rigid bodies with the masses represented by the centre of gravity and mass of inertia. Furthermore, the axis deviation angle of geometric specification is set to zero.

To solve over-determination, the rod system is divided into two substructures. One system is built up of links $Q1$ and $Q2$, and the other of links $Q3$ and $Q4$. The systems are connected by a definable horizontal force. Thus, the forces in the carriages are set to values that the system on the right side presses with a defined horizontal force against the system on the left side. In a second step, gravity, acceleration, and friction forces are added. Based on these results the spindle torque of the NC-drives is calculated. The following figure illustrates the force system.

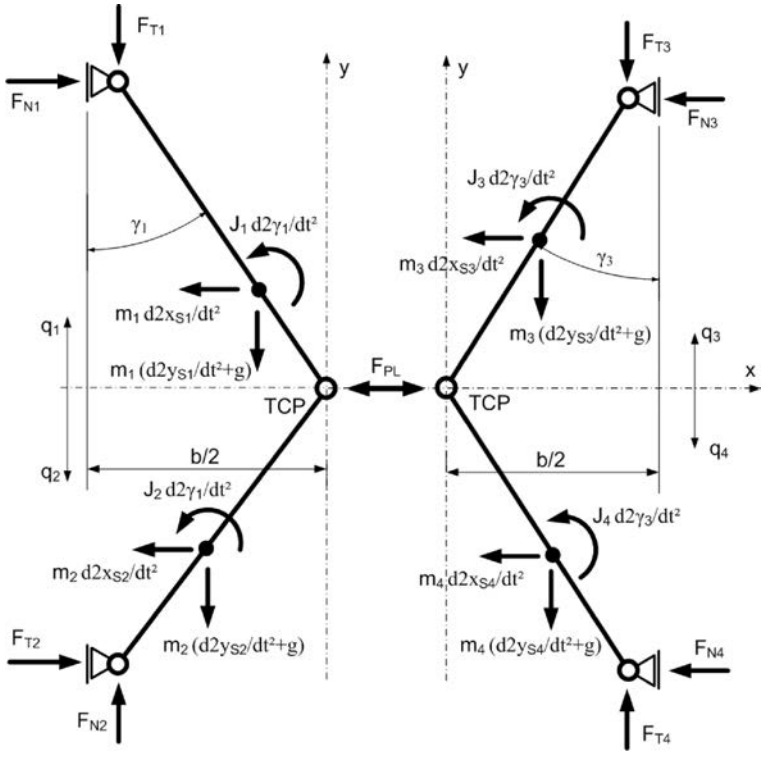

FIG. 7. Parameters for calculation of static and dynamic compensation.

Calculation of the sum of torques in TCP concerning rod $Q1$:

$$J_1\ddot{\varphi}_1 - m_1\ddot{x}_{S1}(l_1 - l_{S1})\cos(\varphi_1) - m_1(\ddot{y}_{S1} - g)(l_1 - l_{S1})\sin(\varphi_1) + F_{T1}l_1\sin(\varphi_1) + F_{N1}l_1\cos(\varphi_1) = 0,$$

$$C_1 = J_1\ddot{\varphi}_1 - m_1\ddot{x}_{S1}(l_1 - l_{S1})\cos(\varphi_1) - m_1(\ddot{y}_{S1} - g)(l_1 - l_{S1})\sin(\varphi_1),$$

$$F_{N1} = -C_1\frac{1}{l_1\cos(\varphi_1)} - F_{T1}\frac{\sin(\varphi_1)}{\cos(\varphi_1)}.$$

Calculation of the sum of torques in TCP concerning rod $Q2$:

$$J_2\ddot{\varphi}_2 - m_2\ddot{x}_{S2}(l_2 - l_{S2})\cos(\varphi_2) + m_2(\ddot{y}_{S2} - g)(l_2 - l_{S2})\sin(\varphi_2) - F_{T2}l_2\sin(\varphi_2) + F_{N2}l_2\cos(\varphi_2) = 0,$$

$$C_2 = J_2\ddot{\varphi}_2 - m_2\ddot{x}_{S2}(l_2 - l_{S2})\cos(\varphi_2) + m_2(\ddot{y}_{S2} - g)(l_2 - l_{S2})\sin(\varphi_2),$$

$$F_{N2} = -C_2\frac{1}{l_2\cos(\varphi_2)} + F_{T2}\frac{\sin(\varphi_2)}{\cos(\varphi_2)}.$$

Force addition of rod $Q1$ and $Q2$:

$$F_{PL} + m_1\ddot{x}_{S1} + m_2\ddot{x}_{S2} - F_{N1} - F_{N2} = 0,$$

$$F_{T2} = \left(F_{PL} + m_1\ddot{x}_{S1} + m_2\ddot{x}_{S2} + C_1\frac{1}{l_1\cos(\varphi_1)} + F_{T1}\frac{\sin(\varphi_1)}{\cos(\varphi_1)}\right)\frac{\cos(\varphi_2)}{\sin(\varphi_2)} + C_2\frac{1}{l_2\sin(\varphi_2)}.$$

Force addition in the Y-direction of rods $Q1$ and $Q2$:

$$m_1(\ddot{y}_S - g) + m_2(\ddot{y}_{S2} - g) - F_{T1} - F_{T2} = 0,$$

$$F_{T1}\left(1 + \frac{\tan(\varphi_1)}{\tan(\varphi_2)}\right) = m_1(\ddot{y}_{S1} - g) + m_2(\ddot{y}_{S2} - g) - \left(F_{PL} + m_1\ddot{x}_{S1} + m_2\ddot{x}_{S2} + C_1\frac{1}{l_1\cos(\varphi_1)}\right)\frac{\cos(\varphi_2)}{\sin(\varphi_2)} + C_2\frac{1}{l_2\sin(\varphi_2)} = 0.$$

Resulting force in the slide system of rod $Q3$:

$$J_3\ddot{\varphi}_3 - m_3\ddot{x}_{S3}(l_3 - l_{S3})\cos(\varphi_3) - m_3(\ddot{y}_{S3} - g)(l_3 - l_{S3})\sin(\varphi_3) + F_{T3}l_3\sin(\varphi_3) + F_{N3}l_3\cos(\varphi_3) = 0,$$

$$C_3 = J_3\ddot{\varphi}_3 + m_3\ddot{x}_{S3}(l_3 - l_{S3})\cos(\varphi_3) - m_3(\ddot{y}_{S3} - g)(l_3 - l_{S3})\sin(\varphi_3),$$

$$F_{N3} = -C_3\frac{1}{l_3\cos(\varphi_3)} - F_{T3}\frac{\sin(\varphi_3)}{\cos(\varphi_3)}.$$

Resulting force in the slide system of rod $Q4$

$$J_4\ddot{\varphi}_4 + m_4\ddot{x}_{S4}(l_4 - l_{S4})\cos(\varphi_4) + m_3(\ddot{y}_{S4} - g)(l_4 - l_{S4})\sin(\varphi_4) - F_{T4}l_4\sin(\varphi_4) + F_{N4}l_4\cos(\varphi_4) = 0,$$

$$C_4 = J_4\ddot{\varphi}_4 + m_4\ddot{x}_{S4}(l_4 - l_{S4})\cos(\varphi_4) + m_3(\ddot{y}_{S4} - g)(l_4 - l_{S4})\sin(\varphi_4),$$

$$F_{N4} = -C_4\frac{1}{l_4\cos(\varphi_4)} + F_{T4}\frac{\sin(\varphi_4)}{\cos(\varphi_4)}.$$

Force addition in the X-direction of rods $Q3$ and $Q4$:

$$F_V - m_3\ddot{x}_{S3} - m_4\ddot{x}_{S4} - F_{N3} - F_{N4} = 0,$$

$$F_{T4} = \left(F_V - m_3\ddot{x}_{S3} - m_4\ddot{x}_{S4} + C_3\frac{1}{l_3\cos(\varphi_3)} + F_{T3}\frac{\sin(\varphi_3)}{\cos(\varphi_3)}\right)\frac{\cos(\varphi_4)}{\sin(\varphi_4)} + C_4\frac{1}{l_4\sin(\varphi_4)}.$$

Force addition in the Y-direction of rods $Q3$ and $Q4$:

$$m_3(\ddot{y}_{S3} - g) + m_4(\ddot{y}_{S4} - g) - F_{T3} - F_{T4} = 0,$$

$$F_{T3}\left(1 + \frac{\tan(\varphi_3)}{\tan(\varphi_4)}\right) = m_3\left(\ddot{y}_{S3} - g + \frac{\ddot{x}_{S3}}{\tan(\varphi_4)}\right) + m_4\left(\ddot{y}_{S4} - g + \frac{\ddot{x}_{S4}}{\tan(\varphi_4)}\right) - \frac{F_V}{\tan(\varphi_4)} - \frac{C_3}{l_3\cos(\varphi_3)\tan(\varphi_4)} - \frac{C_4}{l_4\sin(\varphi_4)}.$$

Consideration of the friction in the carriage:

$$F_{ri} = F_{Ni}\mu_r \cdot \operatorname{sign}(\dot{q}_i).$$

Consideration of the inertial force of the carriage:

$$F_{ai} = m_{Ci}\ddot{q}_i.$$

Calculation of the torque at the drives:

$$T_i = (F_{Ti} + F_{ri} + F_{ai})\frac{h_i}{2\pi\eta_G\eta_S}.$$

5.3. Lag error transfer

To indicate at the force controlled axis a position control, the lag error of the position controlled axis is transferred to the force controlled axis; thus inaccuracies in the geometry are eliminated. As shown in the following figure the transferred lag error can be considered as an input of a P-controller for an additional torque to the axis.

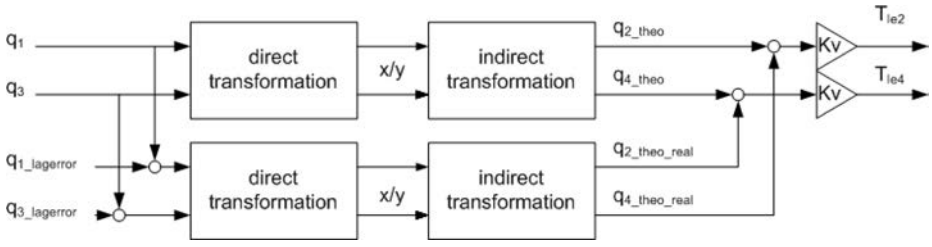

FIG. 8. Lag error transfer.

As a main disadvantage of this method can be observed that the calculation task act as a dead time element with the cyclic time between the input and the calculated output.

6. RESULTS OF EXPERIMENTS

The tests on the real machine were performed by realizing a circular path around the X- and Y-origin with a diameter of 300 mm. The focus of the investigation was to enhance the dynamics of the machine tool (see Fig. 9).

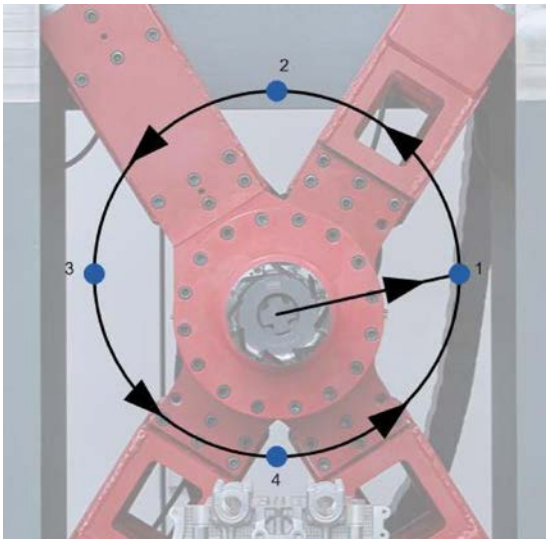

FIG. 9. Test program on the prototype machine.

6.1. Test of control strategy with lag error transfer

In performing tests, in order to investigate the lag error transfer, the axes $Q1$ and $Q2$ were position controlled and the axes $Q3$ and $Q4$ force controlled. The preloading torque was calculated by static compensation as well as the lag error transfer. The constant Kv is the proportional gain with a dimension of Nm/µm.

As presented in Fig. 10 the axis $Q1$ oscillates at the extended position of axes $Q1$ and $Q2$. The lag error transfer prevents this oscillation but causes higher torques on the other drives. Therefore this kind of additional torque eliminates the drive reserves for higher acceleration and movement speed. It is not possible to realize a feed rate of 60 m/min.

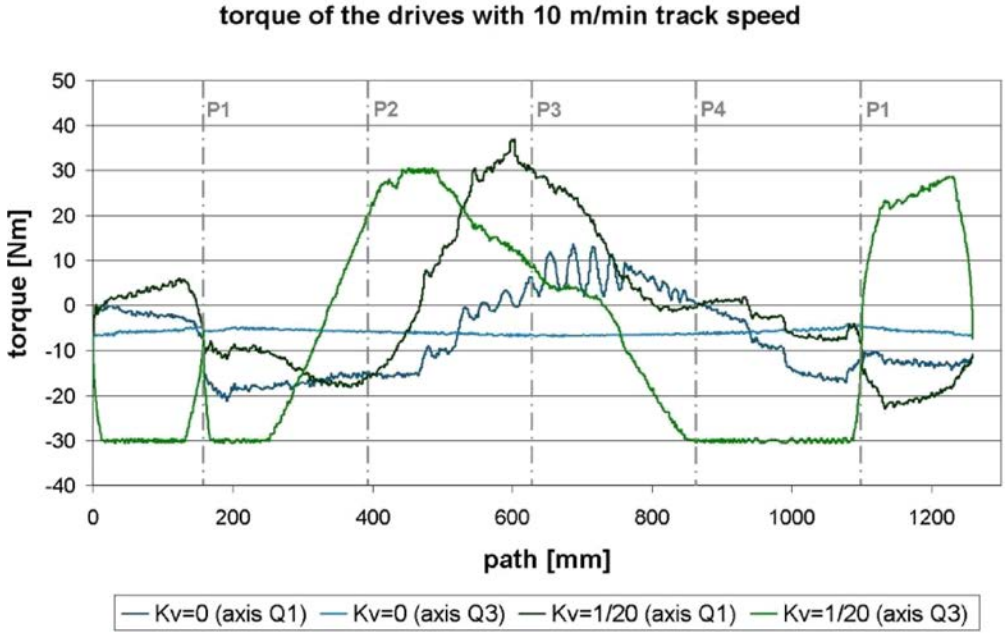

FIG. 10. Torque of the drives with lag error transfer.

6.2. Control Strategy with static and dynamic compensation

To minimize the extended position of the position controlled axis, the axis $Q2$ was replaced by axis $Q3$. Hence it was possible to increase the speed up to 45 m/min.

Figures 11 and 12 show the results of torque measurement of drive $Q1$ and the measured lag error in the XY-plane. At higher path speed the torques and the lag error increase, whereas the oscillation of the values decreases.

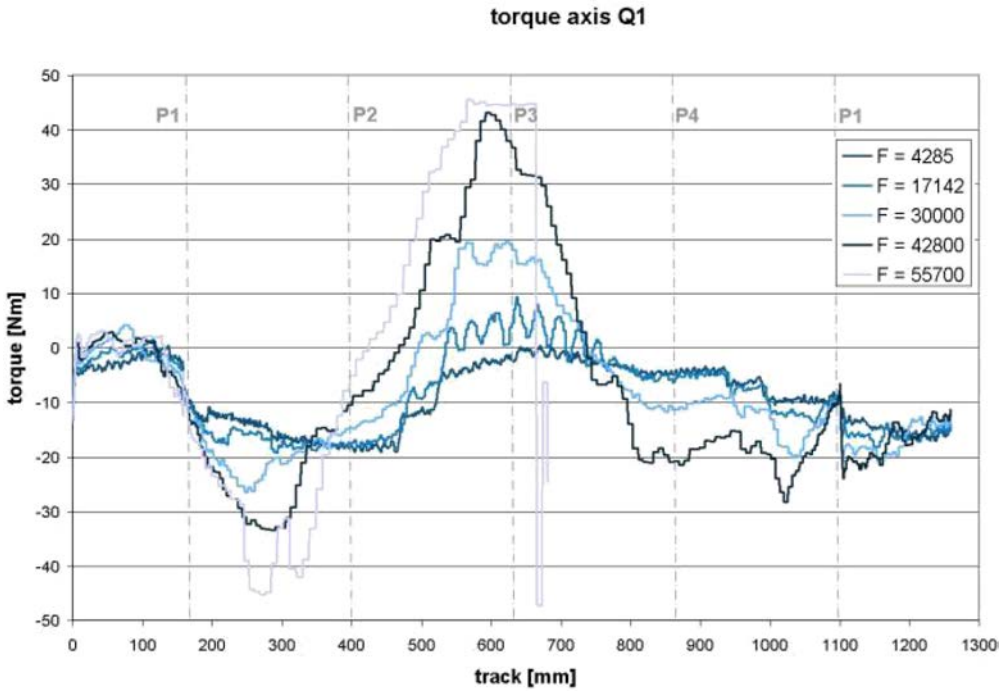

FIG. 11. Torque values measured on axis $Q1$ with different feeding rate.

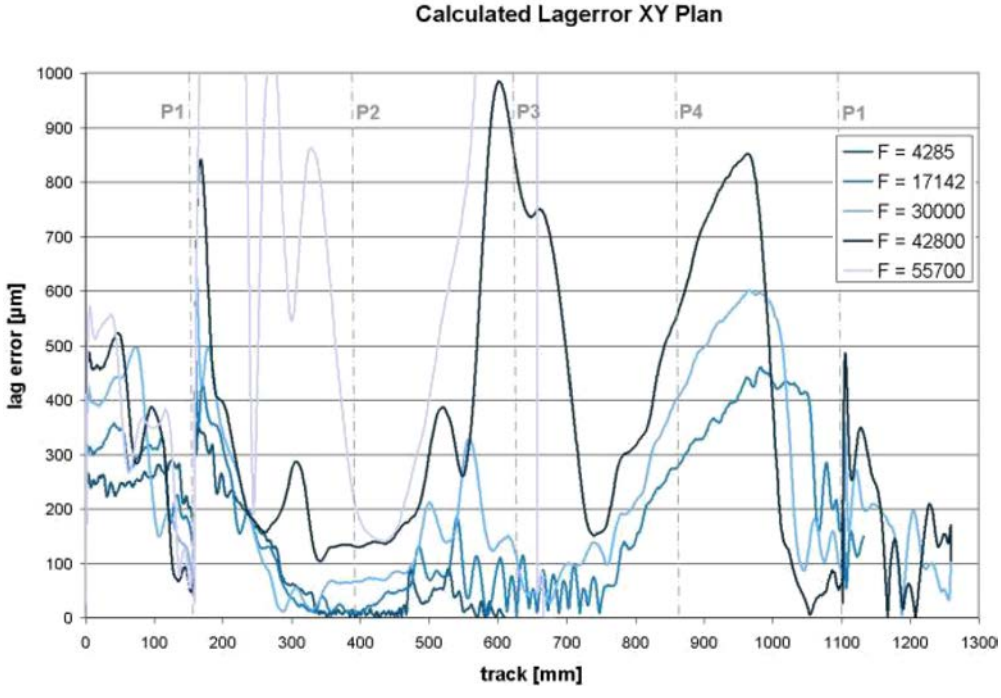

FIG. 12. Measurement results of lag error in the XY-plane with different feeding rate.

6.3. Control strategy comparison

In these tests different strategies focussed on the control implementation of a single axis have been investigated; though as a first step, the 4P-control concept was changed to a 3P1F-control concept. It can be demonstrated that this change in control strategy provides a reduction of the overcharge in the drives due to inaccuracies of the structure.

In Fig. 13 and Fig. 14 it is illustrated that the control concept using three position controlled axes cause at the feed rate of 20 m/min the highest values of measured torques and lag errors.

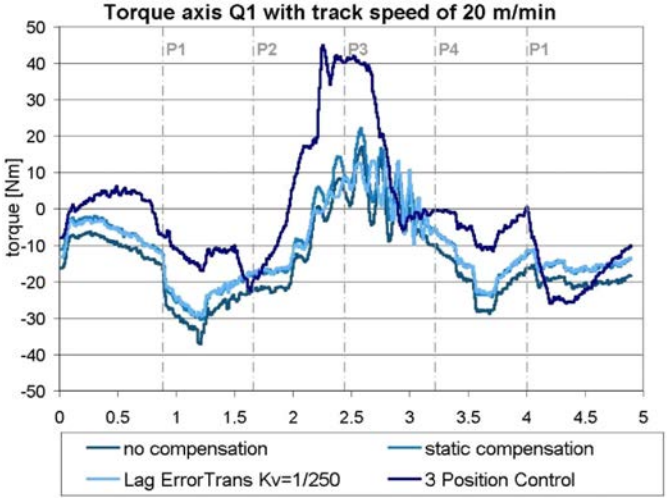

FIG. 13. Measured torque of axis $Q1$ with different strategies.

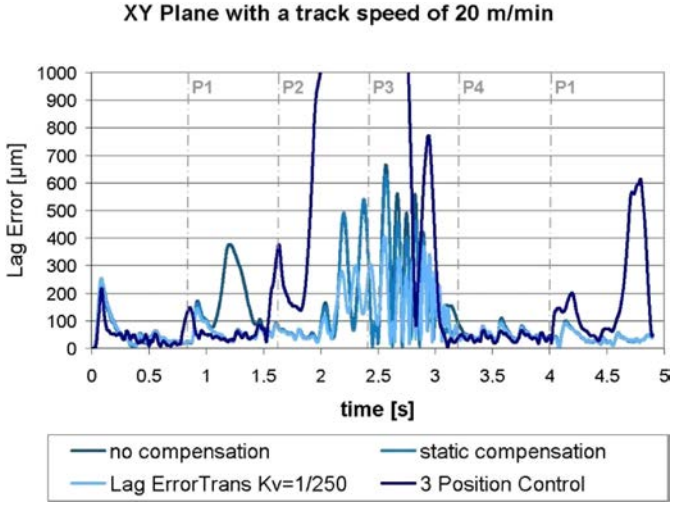

FIG. 14. Measured lag error in the XY-plane with different strategies.

7. Conclusions

The development of a machine tool with a highly parallel kinematics structure comes along with the need of new concepts for compensation of geometrical as well as static and dynamic deviations. Different strategies for compensation and their influence on the position control behavior were investigated. In general the charge of each drive can be reduced by the predefined torques, and thereby higher feed rates and acceleration are possible. Applying a controller strategy using two drives with position control and two drives with force control, oscillations are generated around the extended positions of the driven axes. This effect could be eliminated by a switch of the position dependent axes from one side-pair of struts to the other. The requirement of this change is dependent on the X- and Y-position of the TCP and on which pair of axes is closer to the point of singularity. Using a control strategy with four position controlled axes, nearly oscillation-free motion is possible. The generated drive torques come along with higher values to compensate the restraining forces in the structure. With enhanced predefined torque algorithms it will be possible to distribute the charge uniformly to all axes and increase the maximum feed rate, acceleration, and accuracy.

References

1. Neugebauer R., Stoll A., Kirchner J., Ihlenfeldt S., *Gestaltung, Bewertung und Einsatzerfahrungen von Parallelkinemtiken* [in:] FTK 2000, Stuttgarter Impulse, Technologien für die Zukunft, Stuttgart: Springer-Verlag, p. 316–333, 2000.

2. Neugebauer R., *Parallelkinematische Maschinen*, Springer-Verlag Berlin Heidelberg, ISBN 978-3-5402-9939-4, 2006.

3. Bleicher F., *Parallelkinematische Werkzeugmaschinen*, Neuer wissenschaftlicher Verlag Wien, ISBN 978-3-7083-0118-1, 2003.

4. Bleicher F., *Optimizing a Three-Axes Machine-Tool with Parallel Kinematic Structure*, [in:] Parallel Kinematics Seminar Chemnitz: "Development Methods and Application Experience of Parallel Kinematics", Verlag Wissenschaftliche Scripten Zwickau, Zwickau, p. 883–890, 2002.

5. Mikats T., Puschitz F., Bleicher F., *New Machine Tool Concept 'X-Cut'*, http://www.brautomation.com/files_br_com/Mikats09_New_Machine_Tool_Concept_X-Cut.pdf, 2009.

6. RWTH Aachen, WZL, Presentation site, "HüllerHille – DynaM", http://www.wzl.-rwthaachen.de/de/71b57339ef7396f0c1257792002a55b6.htm, 2011.

7. Beyer L., *Genauigkeitssteigerung von Industrierobotern*, Insbesondere mit Parallelkinematik, Hamburg: Shaker Verlag, 2004.

8. Krüger P., *Innovative Steuerungsalgorithmen für Parallelkinematiken*, [in:] Fortschritt-Bericht VDI, Innovative Werkzeugmaschinen mit Parallelkinematik, Düsseldorf: VDI Verlag GmbH, p. 23–42, 2002.

9. Garber T., Lehner W.-D., *Antriebsregelungen bei Parallelkinematiken*, [in:] Fortschritt-Bericht VDI, Innovative Werkzeugmaschinen mit Parallelkinematik, Düsseldorf: VDI Verlag GmbH, p. 43–58, 2002.

10. Heisel U., Maier W., *DFG SPP 1099 – Production Machines with Parallel Kinematics*, [in:] The 5th Chemnitz Parallel Seminar, Parallel Kinematic Machines in Research and Practice, Zwickau: Verlag Wissenschaftliche Scripten, p. 13–39, 2006.

11. Brecher C., Ostermann T., Friedrich D.A., *Control Concept for PKM Considering the Mechanical Coupling between Actuators*, [in:] The 5th Chemnitz Parallel Seminar, Parallel Kinematic Machines in Research and Practice, Zwickau: Verlag Wissenschaftliche Scripten, p. 413–442, 2006.

12. Bernecker + Rainer Industrie-Elektronik Ges.m.b.H, B&R Product Catalog, Eggelsberg: Bernecker + Rainer Industrie-Elektronik Ges.m.b.H., 2011.

Received April 16, 2012; revised version September 28, 2012.